Biochemical and Biophysical Research Communications 414 (2011) 487–492

Contents lists available at SciVerse ScienceDirect

Biochemical and Biophysical Research Communications

journal homepage: www.elsevier.com/locate/ybbrc

Site directed spin labeling studies of *Escherichia coli* dihydroorotate dehydrogenase N-terminal extension

Sheila G. Couto [a,b], M. Cristina Nonato [c], Antonio J. Costa-Filho [a,d,*]

[a] Instituto de Física de São Carlos, Universidade de São Paulo, Av. Trabalhador São-carlense 400, C.P. 369, 13560-970, São Carlos, SP, Brazil
[b] Grupo de Biofísica e Física Aplicada a Medicina, Instituto de Física, Universidade Federal de Goiás, Campus Samambaia, C.P. 131, 74001-970, Goiânia, GO, Brazil
[c] Laboratório de Cristalografia de Proteínas, Faculdade de Ciências Farmacêuticas de Ribeirão Preto, Universidade de São Paulo, Av. do Café S/N, 14040-903, Ribeirão Preto, SP, Brazil
[d] Departamento de Física, Faculdade de Filosofia, Ciências e Letras de Ribeirão Preto, Av. Bandeirantes 3900, 14040-901, Ribeirão Preto, SP, Brazil

ARTICLE INFO

Article history:
Received 16 September 2011
Available online 2 October 2011

Keywords:
Dihydroorotate dehydrogenase
Membrane association
Electron spin resonance
Vesicles
Site directed spin labeling

ABSTRACT

Dihydroorotate dehydrogenases (DHODHs) are enzymes that catalyze the fourth step of the *de novo* synthesis of pyrimidine nucleotides. In this reaction, DHODH converts dihydroorotate to orotate, using a flavine mononucleotide as a cofactor. Since the synthesis of nucleotides has different pathways in mammals as compared to parasites, DHODH has gained much attention as a promising target for drug design. *Escherichia coli* DHODH (EcDHODH) is a family 2 DHODH that interacts with cell membranes in order to promote catalysis. The membrane association is supposedly made via an extension found in the enzyme's N-terminal. In the present work, we used site directed spin labeling (SDSL) to specifically place a magnetic probe at positions 2, 5, 19, and 21 within the N-terminal and thus monitor, by using Electron Spin Resonance (ESR), dynamics and structural changes in this region in the presence of a membrane model system. Overall, our ESR spectra show that the N-terminal indeed binds to membranes and that it experiences a somewhat high flexibility that could be related to the role of this region as a molecular lid controlling the entrance of the enzyme's active site and thus allowing the enzyme to give access to quinones that are dispersed in the membrane and that are necessary for the catalysis.

1. Introduction

Dihydroorotate dehydrogenase (DHODH) is a flavin-containing enzyme that catalyzes the oxidation of L-dihydroorotate to orotate, the fourth and only redox step in the *de novo* pyrimidine biosynthesis pathway [1]. DHODH has been considered an important target for the design of antiproliferative and antiparasitic agents once inhibition of DHODH leads to reduced levels of pyrimidine precursors which are important for performing a broad range of cellular functions such as cell growth, metabolism and differentiation [2–4].

For DHODHs, the conversion of dihydroorotate to orotate has been described to follow a sequential ping–pong mechanism [5,6]. In the first half-reaction comprising the reduction of dihydroorotate to orotate, electrons are transferred to the flavine mononucleotide moiety (FMN) which becomes oxidized to dihydroflavin mononucleotide ($FMNH_2$). After dissociation of orotate from the enzyme, $FMNH_2$ is regenerated by an appropriate electron receptor.

Based on amino acid sequence similarity, cell location and substrate specificity, DHODHs from different organisms can be divided in two families [1]. Family 1 members are cytosolic enzymes of Gram-positive bacteria, *Archea* and some unicellular eukaryotes, and is further divided into 1A and 1B depending upon their electron receptor and oligomeric state. Family 1A members are dimeric enzymes and utilize fumarate as the electron receptor. Family 1B enzymes form heterotetramers and utilize NAD^+ via a distinct protein subunit that contains a 2Fe–2S cluster and a FAD cofactor [7]. Enzymes of family 2 exist as monomers and are membrane-bound enzymes that utilize quinones as the physiological oxidant during the second half-reaction. The DHODH in family 2 include the enzyme from *Escherichia coli* (EcDHODH), which is attached to the cell membrane [8,9], as well as the enzymes from higher eukaryotes, e.g., *Homo sapiens*, *Plasmodium falcipurum*, which are localized in the inner membrane of mitochondria [10].

DHODHs fold into an α/β barrel with the central barrel of eight parallel β strands surrounded by eight α helices. Two antiparallel β strands are found at the bottom of the barrel, whereas additional secondary structural elements and loops form a protuberant subdomain present at the top of the barrel [11,12]. The prosthetic FMN group is located between the top of the barrel and the subdomain formed by these insertions. In addition to this main barrel, DHODHs of family 2 contain an extra N-terminal domain situated

* Corresponding author at: Departamento de Física, Faculdade de Filosofia, Ciências e Letras de Ribeirão Preto, Av. Bandeirantes 3900, Ribeirão Preto, SP, Brazil.
E-mail address: ajcosta@ffclrp.usp.br (A.J. Costa-Filho).

0006-291X © 2011 Elsevier Inc. Open access under the Elsevier OA license.
doi:10.1016/j.bbrc.2011.09.092

next to the barrel and which folds into two α-helices and one 3_{10} helix [13–15].

Kinetic and structural studies revealed distinct mechanisms for substrate binding when comparing family 1 and 2 DHODHs [16]. Although for all DHODHs the pyrimidine-binding site is found on the si face of the flavin, where the first reductive half-reaction takes place, the oxidative half-reactions for each family are different. In family 1, the dihydroorotate/orotate binding site is also described to be occupied by the oxidant agent [6]. For family 2 members, the N-terminal extension has been proposed to harbor the quinone-binding site, leading the electron acceptor to the FMN cofactor for the redox reaction [13]. This hydrophobic tunnel-like pocket formed by the N-terminal domain has also been found to be the target for drug development [13–17].

To date there is limited information on the mechanism of membrane binding and quinone diffusion in family 2 DHODHs. In our previous work, using *E. coli* DHODH (EcDHODH) as the model system, we have showed that the interaction between family 2 DHODH and model membranes causes a defect-like structure in the membrane hydrophobic region, which is probably the mechanism used by the protein to capture quinones used as electron acceptors during catalysis [18]. In the present work, we have moved forward and investigated the structural changes in the DHODH N-terminal domain in the presence of a membrane model system. To achieve this goal we produced mutants of EcDHODH bearing spin probes in the N-terminal extension. This was done by means of site directed mutagenesis in which a native residue was changed to a cysteine that was in turn specifically labeled with a nitroxide-like probe. This is the basic idea governing the so-called site directed spin labeling technique that, along with ESR experiments, allow one to characterize dynamics and conformational changes occurring during protein function [19–22]. Our results give clear experimental evidences that the N-terminal extension is indeed responsible for the association with the membrane, a paramount step for the enzyme catalysis, and also shed light on the conformational dynamics experienced by that region in presence of the membrane model.

2. Materials and methods

2.1. Materials

1-Dipalmitoyl-2-oleoyl-*sn*-glycero-3-phosphocholine (DOPC) was obtained from Avanti Polar Lipids, Inc. (Birmingham, AL). The sulfhydryl reactive spin-label (1-oxyl-2,2,5,5-tetramethyl-3-pyrroline-3-methyl) methanethiosulfonate (MTSL) was purchased from Toronto Research Chemicals, Inc. (North Fork, ON).

2.2. Construction, expression, purification and spin labeling of EcDHODH mutants

The template EcDHODH gene used for mutagenesis was that coding for the cysteine-free "pseudo-wild-type" protein containing the substitutions C48A, C70A, C158A, and C260A (Mutagenx, NJ). Single cysteine residues were introduced at positions Y2, F5, H19, and F21 of EcDHODH using three-step PCR method. Mutations were confirmed by nucleotide sequencing [23].

EcDHODH mutants were expressed in *E. coli* strain SO6740 [24]. Protein expression was induced by addition of 750 μM isopropyl β-D-thiogalactopyranoside (IPTG). The cells were grown overnight in Luria-Broth medium at 37 °C with vigorous shaking. The cells were collected by centrifugation at 4000*g* for 30 min. EcDHODH mutants were purified as described for the wild-type enzyme [18]. Each EcDHODH mutant was tested to determine whether they were stable and active. The activity test of the EcDHODH mutants was performed as described by Bjornberg et al. [24]. The mutants were then spin labeled with a 10-fold molar excess of the MTSL spin-label after anion exchange chromatography. Spin labeling proceeded overnight at 4 °C under gentle shaking. The unbound label molecules were removed by using dialysis through centrifugal filter devices.

2.3. ESR spectroscopy

Aliquots of a chloroform stock solution of the phospholipid DOPC were dried inside a glass tube by using a nitrogen flow. The dried film was resuspended with the solution containing spin-labeled protein mutants. The final solution for each mutant (50–200 μM) was drawn into a quartz flat cell for ESR experiments. ESR spectra were acquired using a Varian E109 X-band (9.4 GHz) spectrometer. All experiments were carried out at room temperature and several scans were performed to achieve a good signal-to-noise ratio. Experimental parameters were set to avoid saturation and distortions of the final spectrum and included: magnetic field range of 100 G, microwave power of 20 mW, modulation amplitude of 1.0 G.

2.4. NLSL simulations

Non-linear least-squares simulations were performed using the NLLS software, which is based on Freed's developments of the Stochastic Liouville Equation (SLE) [25,26] and implemented in the LabView graphical interface made available by Dr. Christian Altenbach (UCLA) at https://sites.google.com/site/altenbach/labview-programs/epr-programs/multicomponent. The routine solves the SLE for a nitroxide radical undergoing a diffusion motion in a complex fluid and has been successfully applied to a variety of cases [27–29], allowing the calculation of a theoretical ESR spectrum. In terms of parameters, the outputs are: rotational diffusion rates around axes defined in a molecular reference frame and expressed as the components of an R-tensor (in this paper, we used $\bar{R}$ and N that are the components of the tensor in a spherical representation with $\bar{R}$ being the geometric mean $\bar{R} = \bar{R}_x\bar{R}_y\bar{R}_z$ and N the axial rotational anisotropy $N \equiv R_z/\sqrt{R_xR_y}$); order parameter S, calculated from the coefficients of a restoring potential (c20, c22) that governs the diffusion of the probe in a medium with microscopic ordering; line broadenings that can be Gaussian (Δ_G) or Lorentzian (W) and take into account contributions due to inhomogeneous broadenings. All parameters and their definitions are well described in the seminal paper by Budil et al. [26]. The magnetic tensors that describe the Zeeman (g-tensor) and hyperfine (A-tensor) interactions are input parameters taken from the literature in cases where similar structural environments to those found in this work were described. These magnetic parameters are allowed to vary only at the end of the simulation routines as a way of getting the finest adjustment of the experimental spectra. In the cases where a multi-component spectrum is being simulated the program also gives the percentage population for each component.

3. Results and discussions

EcDHODH contains four native cysteine residues that needed to be replaced in order to achieve the specificity required for site directed spin labeling experiments. Hence the first step in our study was to produce a pseudo-native enzyme where each cysteine was mutated to an alanine residue. Previous studies on class2 DHODHs have shown that protein structure and stability are not dependent of N-terminal extension. Truncated versions of malarial DHODH have already been used in order to kinetically characterize the enzyme and search for new inhibitors [30,31]. In fact, the N-terminal

extension in class 2 DHODHs is found to be adjacent to the main core, where the enzymatic mechanism takes place (Fig. 1A). So we do not expect that the exchange of one native residue for a labeled cysteine will dramatically affect the overall structure. Besides, the pseudo-native enzyme maintained native-like activity as evidenced from kinetic assays (see Supplementary material). Starting from this pseudo-native form and to probe the dynamics experienced by the N-terminal extension of EcDHODH, we selectively replaced residues 2, 5, 19, and 21 for cysteines, which were in turn used to label the protein, giving rise to four mutants: Y2R1 and F5R1 located in the beginning of the N-terminal extension, and H19R1 and F21R1 positioned in the second helix of that region (Fig. 1).

Shown in Fig. 2 are the ESR spectra of the Y2R1 and F5R1 EcDHODH mutants incorporated into DOPC/Triton X-100 mixed vesicles. These spectra have been normalized to the same number of spins so that their amplitudes provide an approximate measurement of the dynamics of the spin-label side chain (more mobile spin-labels have larger amplitudes) and, in each case, the shape of the spectrum reflects the motion of the nitroxide on the nanosecond time scale. A qualitative analysis of Y2R1 and F5R1 spectra allows us to infer that both residues experience a high degree of freedom that is compatible with their location in the beginning of the protein chain. Their spectra are typical of residues in loops or in the first turn of a helix with no major structural contacts [32].

The spectra obtained from H19R1 and F21R1 mutants in mixed vesicles are shown in Fig. 3. These clearly show the presence of two spectral components associated with labeled molecules either in a strongly immobilized regime or subjected to a fast motion. The presence of a somewhat high mobility component in these two mutants is surprising due to the fact that they were expected to be located right in the core of the more hydrophobic region of the model membrane. Another interesting feature of H19R1 and F21R1 spectra can be found by simply comparing their lineshapes that point to different degrees of probe mobility even though the labeled positions are just two residues apart from each other.

To further investigate and quantify the dynamic structure observed for each EcDHODH mutant, we used a lineshape analysis based on the non-linear least-squares (NLLS) simulation protocol developed by Freed and co-workers [25,26]. In such a protocol a calculated ESR spectrum is generated by solving the Stochastic Liouville equation for a nitroxide moiety under a classical anisotropic motion and subjected to interactions described by an adequate spin Hamiltonian. In the simulations presented in this paper we used a graphical LabView interface for the original NLSL program as implemented in the software available from Dr. Christian Altenbach website. The simulation procedure allows one to determine parameters that characterize dynamics, expressed as a rotation diffusion rate ($\bar{R}$), and structure, in the form of an order parameter (S).

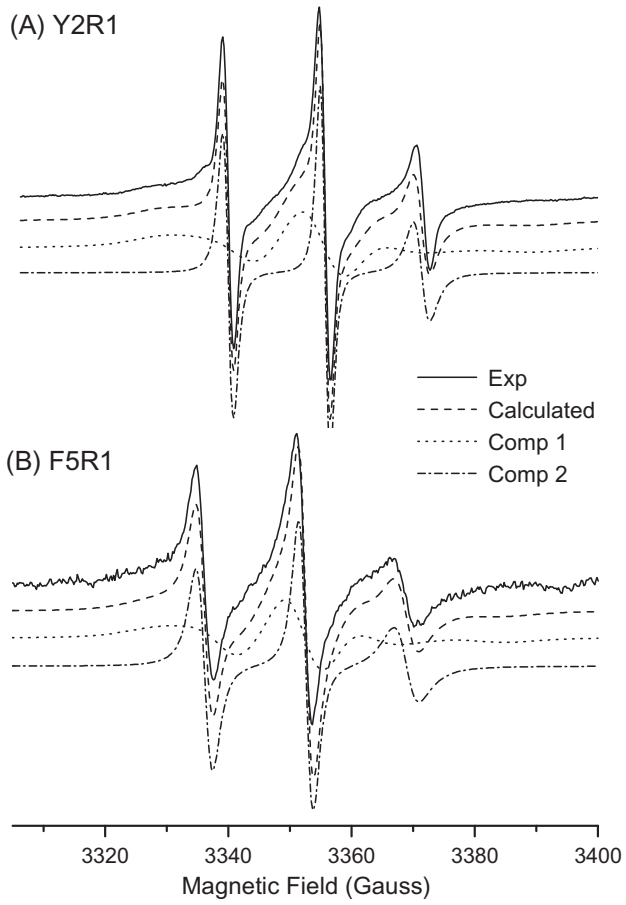

Fig. 2. Room temperature ESR spectra (solid line) along with the best fit (dashed line) from NLSL simulations of the mutants containing the probe at positions Y2 (A) and F5 (B).

The simulations of the spectra obtained from Y2R1 and F5R1 mutants could not be satisfactorily done with the use of only a single component. Several attempts using just one spectral compo-

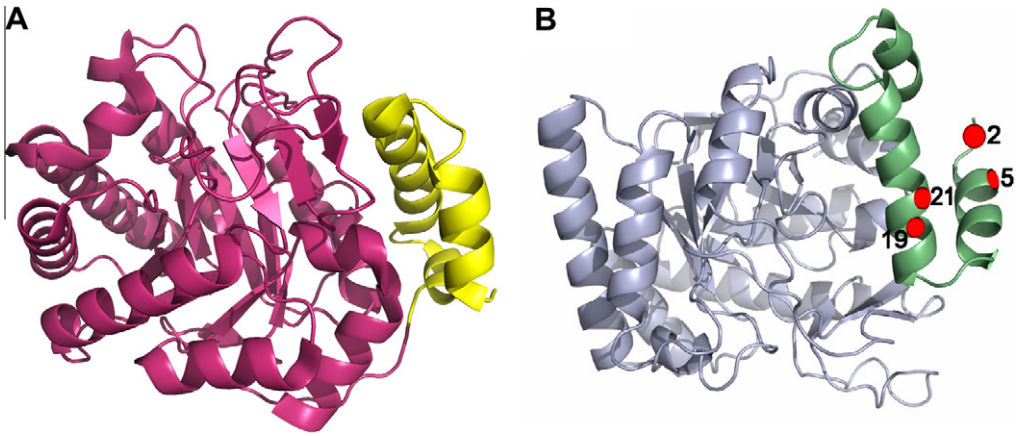

Fig. 1. Overall structure of EcDHODH (PDB ID:1F76) showing: (A) that the N-terminal extension (yellow) and the dihydrogenase domain (magenta) are connected by means of a flexible region; (B) residues used for labeling the protein (red circles). (For interpretation of the references to colour in this figure legend, the reader is referred to the web version of this article.)

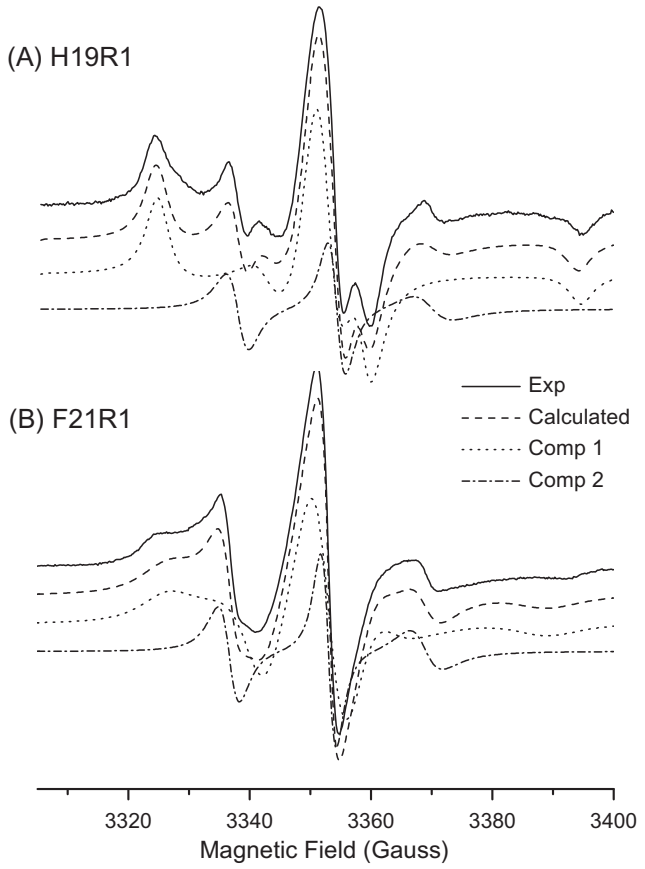

Fig. 3. Room temperature ESR spectra (solid line) along with the best fit (dashed line) from NLSL simulations of the mutants containing the probe at positions H19 (A) and F21 (B).

nent led to poor fitting of the experimental spectra and revealed that the peaks were in fact broader than it could be achieved even when large broadenings were introduced in the simulation routine. This is a clear indication that another species is present and also demonstrates one great advantage of running NLLS simulations, which is the identification of spectral features that would be "invisible" to the naked eye. On the other hand, the ESR spectra of H19R1 and F21R1 (Fig. 3) clearly contain two spectral components and were simulated accordingly. However, the use of more than one component in NLLS simulations always implies the exercise of caution when it comes to defining the number of parameters being used in the calculations. Our strategy to avoid pitfalls was to keep the number of parameters to the minimum needed to produce a reasonable agreement between experimental and theoretical spectra. That required a careful simulation routine where we started calculations using several combinations of dynamics (R components), ordering (c20) and/or broadening mechanisms (Gaussian or Lorentzian). After restarting simulations from several different sets of seed values and taking all precautions described, we determined the set of parameters in Table 1.

From the data for the Y2R1 mutant (Table 1), we can infer that the beginning of the N-terminal region in the presence of the model membrane coexists in two different conformations: one subjected to a more restricted motion (dotted spectrum in Fig. 2A) and a component that shows the fastest motion observed in this region with an $\bar{R}$ value of $0.55 \times 10^9\ s^{-1}$ (dash-dotted spectrum in Fig. 2A). These two states are not equally populated with a preference for the more immobilized species (76%). As for ordering, the Y2R1 parameters show that the fast-motion component does not feel any sort of restoring potential ($S = 0$), while the more immobilized species has an order parameter of 0.33, which indicates an intermediate ordering.

The simulation of the F5R1 spectrum showed the coexistence of two spin probe populations. Unlike Y2R1, the two species now present similar diffusion rates ($\bar{R}$ of $0.36 \times 10^9\ s^{-1}$), but with different degrees of motion asymmetry expressed in the N parameter, which basically represents the ratio in the diffusion rates along the directions of a molecular reference frame constituted by the direction of the NO bond (x-axis), the normal axis to the aromatic ring containing the nitroxide moiety (z-axis) and a direction that makes an orthogonal system with the x and z. An either very low or null restoring potential was needed for the simulations of the two components. Hence, we can infer that the components detected at position 5 of the polypeptide chain in the presence of the model membrane have very little orienting preferences and both undergo a fast motion but with different degrees of anisotropy.

In the case of the H19R1 spectrum, although it clearly contains two spectral components (Fig. 3A), the parameters in Table 1 indicate that one of those species is low populated (13%), characterized by a very fast motion with no ordering and a very high average hyperfine splitting [$A_0 = (A_x + A_y + A_z)/3 = 16.6$ G]. A_0 values are used as a measure of the polarity around the spin label moiety with high values (above ca. 16 G) representing polar environments. This information suggests that such component must be due to a spin label population that did not react with the cysteine residues and could not be completely removed during the enzyme purification. The second component, on the other hand, is characterized by slow motion ($\bar{R} = 0.42 \times 10^7\ s^{-1}$) and very high ordering ($S = 0.91$) of the spin probe at position 19, indicating that this part of the polypep-

Table 1
Parameters obtained from NLSL simulations of the EcDHODH mutants.

	Y2R1		F5R1		H19R1		F21R1	
	1	2	1	2	1	2	1	2
A_{xx}	6.2	6.2	6.2	6.2	6.9	5.6	5.5	6.2
A_{yy}	5.9	5.9	5.9	5.9	5.0	5.0	5.5	5.9
A_{zz}	37.8	35.2	35.5	37.5	35.4	39.2	38.8	37.8
g_{xx}	2.0076	2.0076	2.0076	2.0076	2.0078	2.0078	2.0081	2.0067
g_{yy}	2.0050	2.0050	2.0050	2.0050	2.0058	2.0055	2.0046	2.0055
g_{zz}	2.0023	2.0023	2.0023	2.0023	2.0019	2.0023	2.0015	2.0029
$\bar{R}$	0.85×10^8	0.55×10^9	0.36×10^9	0.35×109	0.42×10^7	0.72×10^9	0.42×10^8	0.95×10^9
N	0.31	0.47	1.19	0.42	0.36	1.00	0.69	1.15
S	0.33	–	0.01	–	0.91	–	0.29	–
%	76	23	59	41	87	13	83	17

Hyperfine tensor components are in Gauss and $\bar{R}$ values are in s^{-1}.
Estimated errors: $\bar{R}$ (5%), A_{zz} (5%), N (10%).

tide chain assumes a very rigid and well-oriented configuration in the presence of the model membrane system.

Finally, the spectrum of the F21R1 mutant also shows two spectral components with one of them attributable to free spin label (component 2 in Table 1). The other component is associated with spin probes in a slow motion regime but, unlike the H19R1 case, with relatively low ordering ($S = 0.29$). Hence, at this position, the probe undergoes an intermediate rotational diffusion ($\bar{R} = 0.42 \times 10^8\ s^{-1}$) with larger amplitude than it was observed for H19R1. The nitroxide experiences several different orientations in a somewhat longer time scale. This situation is probably the result of a less tightly packed arrangement of the helix at position 21 than 19.

Taking together the information discussed above we can say that the N-terminal region of EcDHODH in the presence of a model membrane system is characterized by:

(1) Coexistence of two conformations in the first helix of the region as inferred from the ESR spectra and simulations obtained for the Y2R1 and F5R1 mutants (Fig. 2 and Table 1). This helix is more flexible (higher rotational diffusion rates) and with larger amplitude motions (lower ordering parameters) than the other helix that composes the N-terminal domain.
(2) The second helix of the N-terminal domain is in a more rigid conformation. However, the dynamics and ordering experienced by residues 19 and 21 are distinct and point to a very well-defined orientation of the side chain of residue 19 as compared to residue 21. This is in agreement with what would be expected from the protein crystal structure [15], where it is seen that residue 19 points inwards (facing the protein's interior) while residue 21 assumes an orientation with its side chain in a less packed structural environment.

The co-existence of conformations in helix 1 and the low ordering experienced by the probe at position 21 suggest that the N-terminal extension is flexible enough to undergo an open/close structural transition with helix 1 being the region with larger amplitude and faster motions, whereas helix 2 would be more tightly packed against the protein structure. The swapping observed for residues 2 and 5 between a more mobile and a more immobile conformation is compatible with an open/close structural transition where the more immobile component is the one adopted in the closed state and is likely to bring the residue side chain in closer proximity with the protein inside, whereas the more flexible species is associated with the helix experiencing a much less restricted motion due to its location farther away from the protein structural elements and in contact with the less packed mixed micelle interior, which would then allow for the higher dynamics observed in the ESR spectra of Y2R1 and F5R1. This flexibility guarantees that the N-terminal domain would work as a sort of lid that controls the access to the β-barrel domain, where the enzyme's active site is located. We believe that this would be the mechanism used by the protein to fish out the quinones, which act as electron acceptors and that are dispersed in the membrane, and then conduct the enzymatic catalysis. Our results shed light on the molecular mechanism used by EcDHODH to convert dihydroorotate to orotate and, to the best of our knowledge, are the first experimental evidence showing that the N-terminal region interacts with membranes and, furthermore, it exerts a major role during catalysis.

Acknowledgments

The authors thank the Brazilian agencies FAPESP and CNPq for financially supporting this work. The authors are grateful to Prof. K. F. Jensen who kindly provided the PAG1 plasmid and *E. coli* cell strain S06740 used for EcDHODH expression and to Dr. Christian Altenbach who provided the Labview interface for the simulation program.

Appendix A. Supplementary data

Supplementary data associated with this article can be found, in the online version, at doi:10.1016/j.bbrc.2011.09.092.

References

[1] O. Bjornberg, P. Rowland, S. Larsen, K.F. Jensen, Active site of dihydroorotate dehydrogenase A from Lactococcus lactis investigated by chemical modification and mutagenesis, Biochemistry 36 (1997) 16197–16205.
[2] R.I. Fox, M.L. Herrmann, C.G. Frangou, G.M. Wahl, R.E. Morris, V. Strand, B.J. Kirschbaum, Mechanism of action for leflunomide in rheumatoid arthritis, Clin. Immun. 93 (1999) 198–208.
[3] R.A. Williamson, C.M. Yea, P.A. Robson, A.P. Curnock, S. Gadher, A.B. Hambleton, K. Woodward, J.M. Bruneau, P. Hambleton, D. Moss, T.A. Thomson, S. Spinella-Jaegle, P. Morand, O. Courtin, C. Sautés, R. Westwood, T. Hercend, E.A. Kuo, E. Ruuth, Dihydroorotate Dehydrogenase Is a High Affinity Binding Protein for A77 1726 and Mediator of a Range of Biological Effects of the Immunomodulatory Compound, J. Biol. Chem. 270 (1995) 22467–22472.
[4] M.L. Herrmann, R. Schleyerbach, B.J. Kirschbaum, Leflunomide: an immunomodulatory drug for the treatment of rheumatoid arthritis and other autoimmune diseases, Immunopharmacology 47 (2000) 273–289.
[5] P.R. Feliciano, A.T. Cordeiro, A.J. Costa, M.C. Nonato, Cloning, expression, purification, and characterization of Leishmania major dihydroorotate dehydrogenase, Protein, Expression Purif. 48 (2006) 98–103.
[6] D.K. Inaoka, K. Sakamoto, H. Shimizu, T. Shiba, G. Kurisu, T. Nara, T. Aoki, K. Kita, S. Harada, Structures of trypanosoma cruzi dihydroorotate dehydrogenase complexed with substrates and products: atomic resolution insights into mechanisms of dihydroorotate oxidation and fumarate reduction, Biochemistry 47 (2008) 10881–10891.
[7] P.S. Andersen, P.J.G. Jansen, K. Hammer, Different dihydroorotate dehydrogenases in Lactococcus lactis, J. Bacteriol. 176 (1994) 3975–3982.
[8] D. Karibian, Dihydroorotate dehydrogenase (*Escherichia coli*), Methods Enzymol. 51 (1978) 58–63.
[9] J.N. Larsen, K.F. Jensen, Nucleotide sequence of the pyrD gene of Escherichia coli and characterization of the flavoprotein dihydroorotate dehydrogenase, Eur. J. Biochem. 151 (1985) 59–65.
[10] W. Knecht, U. Bergjohann, S. Gonski, B. Kirschbaum, M. Loffler, Functional expression of a fragment of human dihydroorotate dehydrogenase by means of the baculovirus expression vector system, and kinetic investigation of the purified enzyme, Eur. J. Biochem. 240 (1996) 292–301.
[11] M.P. Pinheiro, J. Iulek, M.C. Nonato, Crystal structure of Trypanosoma cruzi dihydroorotate dehydrogenase from Y strain, Biochem. Biophys. Res. Commun. 369 (2008) 812–817.
[12] S. Norager, S. Arent, O. Bjornberg, M. Ottosen, L. Lo Leggio, K.F. Jensen, S. Larsen, Lactococcus lactis dihydroorotate dehydrogenase A mutants reveal important facets of the enzymatic function, J. Biol. Chem. 278 (2003) 28812–28822.
[13] S.P. Liu, E.A. Neidhardt, T.H. Grossman, T. Ocain, J. Clardy, Structures of human dihydroorotate dehydrogenase in complex with antiproliferative agents, Struct. Fold. Des. 8 (2000) 25–33.
[14] D.E. Hurt, J. Widom, J. Clardy, Structure of Plasmodium falciparum dihydroorotate dehydrogenase with a bound inhibitor, Acta Crystallogr., Sect. D: Biol. Crystallogr. 62 (2006) 312–323.
[15] S. Norager, K.F. Jensen, O. Bjornberg, S. Larsen, *E-coli* dihydroorotate dehydrogenase reveals structural and functional distinctions between different classes of dihydroorotate dehydrogenases, Structure 10 (2002) 1211–1223.
[16] M. Hansen, J. Le Nours, E. Johansson, T. Antal, A. Ullrich, M. Loffler, S. Larsen, Inhibitor binding in a class 2 dihydroorotate dehydrogenase causes variations in the membrane-associated N-terminal domain, Protein Sci. 13 (2004) 1031–1042.
[17] S. Norager, K.F. Jensen, O. Bj€ornberg, S. Larsen, Structures of human dihydroorotate dehydrogenase in complex with antiproliferative agents, Structure 8 (2002) 25–33.
[18] S.G. Couto, M.C. Nonato, A.J. Costa-Filho, Defects in vesicle core induced by Escherichia coli dihydroorotate dehydrogenase, Biophys. J. 94 (2008) 1746–1753.
[19] G.E. Fanucci, D.S. Cafiso, Recent advances and applications of site-directed spin labeling, Curr. Opin. Struct. Biol. 16 (2006) 644–653.
[20] C. Altenbach, S.L. Flitsch, H.G. Khorana, W.L. Hubbell, Structural studies on transmembrane proteins. 2 Spin labeling of bacteriorhodopsin mutants at unique cysteines, Biochemistry 28 (1989) 7806–7812.
[21] L. Columbus, W.L. Hubbell, A new spin on protein dynamics, TIBS 27 (2002) 288–295.
[22] W.L. Hubbell, D.S. Cafiso, C. Altenbach, Identifying conformational changes with site-directed spin labeling, Nat. Struct. Biol. 7 (2000) 735–739.

[23] R. Sanger, S. Nicklen, A.R. Coulson, DNA Sequencing with Chain-Terminating Inhibitors, Proc. Nat. Acad. Sci. USA 74 (1977) 5436–5467.

[24] O. Bjornberg, A.C. Gruner, P. Roepstorff, K.F. Jensen, The activity of Escherichia coli dihydroorotate dehydrogenase is dependent on a conserved loop identified by sequence homology, mutagenesis, and limited proteolysis, Biochemistry 38 (1999) 2899–2908.

[25] D.J. Schneider, J.H. Freed, Calculating slow motional magnetic resonance spectra: a user's guide, in: L.J. Berliner, J. Reuben (Eds.), Biological Magnetic Resonance, Plenum Publishing, New York, 1989, pp. 1–76.

[26] D.E. Budil, S. Lee, S. Saxena, J.H. Freed, Nonlinear-least squares analysis of slow-motion EPR spectra in one and two dimensions using a modified Levenberg-Marquardt algorithm, J. Magn. Reson. A120 (1996) 155–189.

[27] L. Columbus, W.L. Hubbell, Mapping backbone dynamics in solution with site-directed spin labeling: GCN4-58 bZip free and bound to DNA, Biochemistry 43 (2004) 7273–7287.

[28] A.P.S. Citadini, A.P.A. Pinto, A.P.U. Araújo, O.R. Nascimento, A.J. Costa-Filho, EPR studies of chlorocatechol 1 2-dioxygenase: Evidences of iron reduction during catalysis and of the binding of amphipatic molecules, Biophys. J. 88 (2005) 3502–3508.

[29] M.T. Ge, A. Gidwani, H.A. Brown, D. Holowka, B. Baird, J.F. Freed, Ordered and disordered phases coexist in plasma membrane vesicles of RBL-2H3 mast cells, Biophys. J. 85 (2003) 1278–1288.

[30] J. Baldwin, A.M. Farajallah, N.A. Malmquist, P.K. Rathod, M.A. Phillips, Malarial dihydroorotate dehydrogenase. Substrate and inhibitor specificity, J. Biol. Chem. 277 (2002) 41827–41834.

[31] N.A. Malmquist, J. Baldwin, M.A. Phillips, Detergent-dependent kinetics of truncated plasmodium falciparum dihydroorotate dehydrogenase, J. Biol. Chem. 282 (2007) 12678–12686.

[32] H.S. Mchaourab, T. Kálai, K. Hideg, W.L. Hubbell, Motion of spin-labeled side chains in t4 lysozyme: effect of side chain structure, Biochemistry 38 (1999) 2947–2955.